Fault Detection Experiment of Unbalanced Voltage and Air Gap Eccentricity on Induction Motor Using a Flux Sensor

Nurul Husnah
Department of Electrical Engineering
Institut Teknologi Sepuluh Nopember
Surabaya, Indonesia
nunurul.email@gmail.com

Dimas Anton Asfani
Department of Electrical Engineering
Institut Teknologi Sepuluh Nopember
Surabaya, Indonesia
anton@ee.its.ac.id

I Made Yulistya Negara
Department of Electrical Engineering
Institut Teknologi Sepuluh Nopember
Surabaya, Indonesia
yulistya@ee.its.ac.id

***Abstract*— The induction motor is one of the popular equipment used in various types of industrial sectors. It is necessary to monitor the condition of the induction motor to maintain its safety and performance of the induction motor. The most common damage to the induction motor is bearing failure reaches 40% resulting in air gap eccentricity. Most of the research to detect the occurrence of air gap eccentricity is carried out based on the analysis of motor current signals. To overcome the disadvantages of the above methods, the detection of air gap eccentricity using a sensor flux that can detect leakage flux from the motor body and the fault detection results by measuring the flux signal analyzed. Flux analysis using the Fast Fourier Transform (FFT) algorithm in balanced and unbalanced voltage conditions. Induction motor failure analysis compared normal motor conditions with an eccentricity of 0.1 mm and 0.2 mm. Eccentricity detection is done by monitoring the amplitude that emerges in the frequency spectrum with notice of the threshold. Detection results from the eccentricity fault showed that success is detected 100% using a sensor flux on unbalanced voltage (under voltage 5%) at a full-load condition.**

Keywords— Unbalanced Voltage, Eccentricity, Flux Sensor, Induction Motor, Fast Fourier Transform (FFT).

I. INTRODUCTION

One of the ordinary electric motors used in many applications is the induction motor. Therefore, its performance considerably affects the productivity of an industry. Several factors affect the performance of induction motors, one of which is unbalanced voltage. Another factor capable of causing accelerated motor failure is the air gap unbalance [1].

The fault in the machine is usually detected by monitoring high-frequency vibrations and current terminal components over a prolonged period. These strategies can be used to detect rotor eccentricity due to incorrect bearing position during assembly, worn bearings, bent rotor shaft, and operation at critical speeds, which causes rotor "swirl" [2]. Therefore, installing a flux sensor on the motor is necessary to determine the effect of voltage imbalance and air gap early. Meanwhile, the state of eccentricity can be identified directly by measuring the change in magnetic flux using a specially designed magnetic flux sensor [3].

The fluxgate magnetic sensor is based on the characteristics of a linear ferromagnetic core and has high linearity and sensitivity [4]. The *stray flux* sensor [5] has been used to detect inter-turn short circuits in three-phase induction machines. In addition, it efficiently notices stator winding faults in the low-frequency range and resolution of the flux spectrum [10]. Frequency resolution is used to set the level of accuracy for amplitude observations in the spectrum. Stator current signal frequency analysis using FFT is the most popular method for detecting rotor errors in induction motors [6].

The preliminary study by Don-Ha Hwang et al. determined the effect of air gap imbalance on the performance of electric motors using a flux sensor [3], and It examined the eccentricity and damaged condition of the rotor rod in a squirrel-cage induction motor using the finite element method with the air gap flux. This is similar to the study by R. Romary et al. [7], which used spectral lines matching the slotting effect to determine the harmonics in the engine air gap. However, didn't compare it with the effect of load and unbalanced voltage. O. Vitek, M. Janda, and V. Hajek, P. Bauer [8] described detecting rotor eccentricity and diagnosing faults using the magnetic flux density method. The equipment used for stray flux measurement, the tesla meter Bell 7030, is very expensive for practical utilization in industrial applications, especially when the small induction motors are taken into account. The rotor eccentricity detection of the induction motor is represented by dynamic eccentricity.

Therefore, this research will be developed using the static air gap eccentricity in which the motor experiences an unequal air gap parallel to the rotor and stator. The detection of eccentricity disturbances with flux sensors using the FFT algorithm method on harmonics that appear at several frequencies, and detection results from measuring the flux signal optimal fault detection is obtained when the unbalanced voltage supplies on various loaded conditions.

II. BASIC THEORY

A. The Air Gap Excentricity

The air gap is a space between the stator and rotor, which functions as a place for the flow of flux from the magnetic field generated by the stator coil. When the air gap between the stator and the rotor is too large, it will lead to low motor efficiency. However, when the air gap is too small, it causes mechanical damage to the engine.

The cause of the asymmetrical air gap between the rotor and stator is called eccentricity. This process can occur in two forms, namely static (does not change with time) and dynamic (changes with time). Examples of static eccentricity are the

How to cite: Husnah, N., Asfani, D. A., & Negara, I. M. Y (2023). Fault Detection Experiment of Unbalanced Voltage and Air Gap Eccentricity on Induction Motor Using a Flux Sensor. *JAREE (Journal on Advanced Research in Electrical Engineering), 7(1).*

occurrence due to the non-roundness of the stator or the rotor axis, which is not in line with the stator axis Meanwhile, dynamic eccentricity occurs due to the irregularity of the rotor [9]. In several studies, eccentricity in the air gap is caused by damage to the bearing components. Damage to the outer bearing can cause static eccentricity because the external ring does not rotate with the rotor. The static eccentricity damage is the same as those on the outer ring [11].

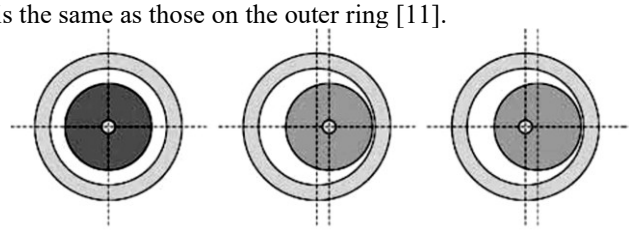

(a) (b) (c)

Fig. 1. Air gap: (a) normal, (b) static eccentricity, (c) dynamic eccentricity

In the case of static eccentricity, the sideband components appear at the frequency specified in the existing equation [1].

$$f_e = f_s \pm k f_r \quad (1)$$

Where,

$$f_r = f_s\left(\frac{1-s}{p}\right) \quad (2)$$

Furthermore, f_r is the rotor frequency, f_s is the fundamental frequency, slip and p are pairs of poles.

$$S = \frac{Ns-NR}{NR} \quad (3)$$

Ns is the stator speed and N_R is the rotor speed.

The eccentricity of the air gap in an induction motor gives rise to the appearance of an additional component in the motor supply current spectrum, the frequency of which is given by [13]

$$f_{ecc} = f_s\left[(nR \pm n_e)\left(\frac{1-s}{P}\right) \pm n_{ws}\right] \quad (4)$$

Where n = 0, 1, 2, ..., R is the number of rotor slots, p is the number of pole pairs, n_e is the eccentricity order number (n_e = 0 for the static eccentricity case; n_e = 1, 2, ... for dynamic eccentricity) and n_ws is the time-harmonic sequence the number of the MMF stator (n_{ws} = 1, 2, 3,…).

B. The Flux Sensor

Fluxgate magnetic sensor is based on the characteristics of a linear ferromagnetic core. In the simplest form, it consists of two coils, the primary and secondary, which are used for excitation and pick-up [12]. The sensor sensitivity can be increased by raising the number of secondary coil turns in line with Faraday's law of induction [4].

In this study, the leakage flux was detected using an ELF Gauss meter type IDR-210, as shown in Fig. 2. The instrument of Gauss meter device is useful for measuring the strength of the magnetic field around the device. It comprises a sensor connected by a cable to the monitor, whose function is to determine the magnetic field.

Fig. 2. ELF Gauss Meter type IDR-210

C. Unbalanced Voltage

The National Electrical Manufacturers Association (NEMA) and International Electrotechnical Commission (IEC) standards introduced definitions for unbalanced voltage and one of them is used to analyze electrical machines. The Voltage Unbalance Percentage (VUP) at the machine terminals, based on the definition of NEMA can be expressed as follows [1].

The unbalance voltage is defined as:

$$Vun = \frac{Vdev}{Vavg} \text{x} 100 \quad (5)$$

Where, V_{un} is the unbalanced voltage in percent, V_{dev} is the deviation of magnitude maximum voltage and V_{avg} is the average magnitude of voltage.

III. Experimental Setup

A. The Experiment Configuration

The system configuration in this study is shown in Fig.3. The power supply was used to perform an induction motor. The process of measuring the stator current using the NI DAQ-9246 and the leakage flux using a flux sensor connected to the NI DAQ-9775 for voltage data acquisition. The mechanical loading of the induction motor is carried out by coupling the induction motor with a 3-phase synchronous generator loaded with several lamps, and regulating the supply voltage using a voltage *variac*. *Labview* software is integrated with the NI DAQ-9246 and NI DAQ-9775 to make sampling frequency selection easier. The measurement results will be processed using the FFT method with *DIAdem* and *MATLAB* software.

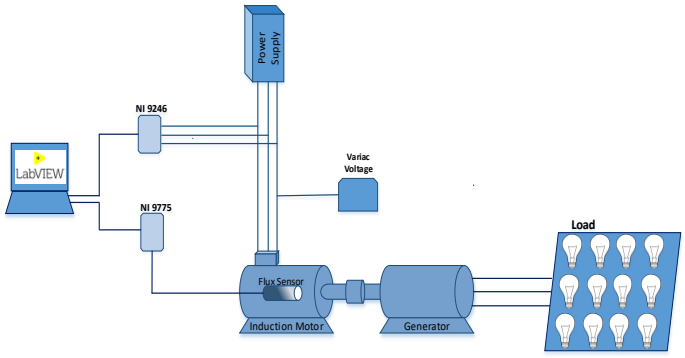

Fig. 3. Experimental configuration system

The specifications for a 3-phase induction motor can be seen in Table 1 below.

TABLE I. INDUCTION MOTOR SPECIFICATION

ADK Electric Motor			
Power		1.5 kW	2 HP
No.	Y3192058	Type	Y3-90L-4
V	220 / 380	Amb.	40 C°
A	6.36 / 3.68	Speed	1400 rpm
IP	55	Freq.	50 Hz
Ins.	CL F	Weight	23 Kg

B. Recondition of Bearing

In this study, the eccentricity was made with a defect level of 0.1 mm and 0.2 mm. This process was carried out because the maximum air gap is only 0.25 mm on both sides under normal conditions. In reconstructing the air gap on an induction motor [14], it is helpful to look at the normal bearing sizes, which are used as a reference to align the size with the asymmetrical rotor rotation. The bearing has a size with outer and inner diameters of 52 mm and 25 mm, respectively. The size of the normal bearing was changed to outer and inner diameters of 47 mm and 25 mm, respectively, to make the rotor unsuitable. Furthermore, a more precise bearing is obtained by installing it on the original bearing housing, which is misaligned on a ring with outer and inner diameters of 52 mm and 47 mm, respectively. The ring is then placed on a coat with smaller bearing replacements to ensure the same size as the original. Finally, to make the rotor shaft asymmetrical or eccentric, the thickness of the ring bearings is made differently. The results of bearing sizes are shown in Fig. 4.

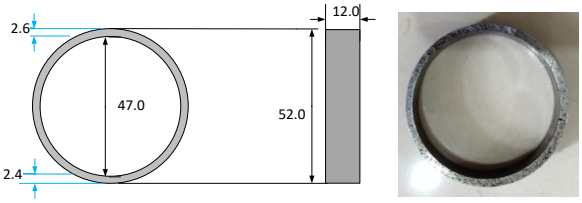

Fig. 4. Rings with different thicknesses

The ring thickness is used to coat the bearing, which is 2.6 mm and 2.4 mm thick on the top and bottom, with a shaft shift of 0.1 mm. This makes the width of the air gap unbalanced. This study was carried out using the static air gap eccentricity in which the motor experiences an unequal air gap parallel to the rotor and stator. The installation of a ring with different thicknesses and aligned bearings is shown in Fig. 5.

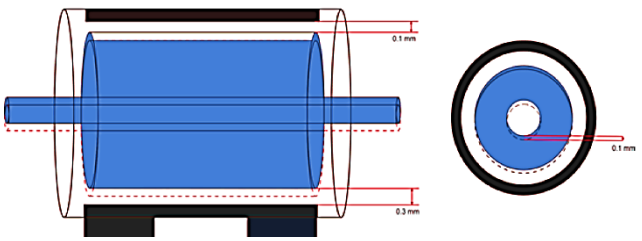

Fig. 5. Eccentricity of air gap with movement cylinder rotating.

Fig. 6 presents the comparison between normal and smaller bearing sizes with ring of different thicknesses used in this study.

(a) (b)

Fig. 6. a) Comparison of normal bearing sizes with replacement bearings, b) Replacement bearings with eccentric rings.

IV. EXPERIMENTAL TEST AND RESULT

The test was carried out by comparing the results of frequency spectrum analysis on normal motors and air gap eccentricity conditions with balanced and unbalanced voltage supplies. The condition of the air gap eccentricity is made with two levels of damage, that is 0.1 mm and 0.2 mm. This is intended to determine the effect of the level of eccentricity on changes in the frequency spectrum. Furthermore, this process is also carried out under loaded conditions to improve the accuracy of the analysis process and determine the effect of loading on the results of the air gap eccentricity detection analysis through the frequency resolution of the leakage flux. Loading conditions are made into three different types, namely no-load, half-load, and full-load.

TABLE II. EXPERIMENT SCHEME

Motor condition	Normal	Fault 1 (eccentricity 0.1 mm)	Fault 2 (eccentricity 0.2 mm)
Load (%)	0% 50% 100%	0% 50% 100%	0% 50% 100%
Voltage case	▪ Balance ▪ Unbalance voltage		

In this study, the limited number of frequencies observed is limited to 0 Hz-1000 Hz. The frequency was selected to determine where the most sensitive frequency is located from <500 Hz to >500 Hz.

An example of the results of the FFT is shown in Fig. 7. From the simulation results using *Matlab*, the frequency limit that needs to be displayed is determined, which enables the harmonic amplitude values to be plotted and analyzed.

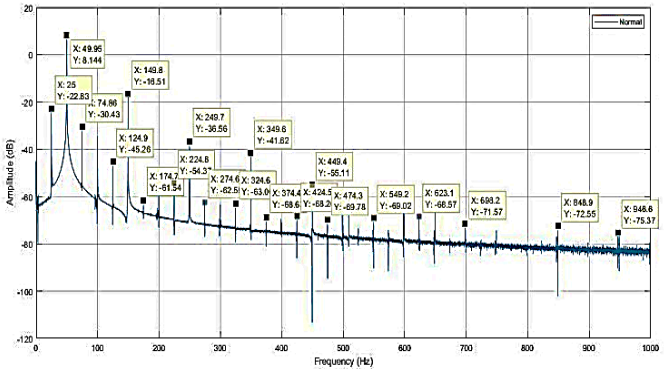

Fig. 7. FFT simulation results using Matlab

The following is a comparison of the frequency spectrum between the motor under normal and faulty conditions. From Fig. 8, it can be seen that the interference detection spectrum is more sensitive at low frequencies of 0 Hz - 500 Hz. Therefore, the data to be analyzed is displayed using harmonic ranks of 1, 3, 5, 7, and 9 at frequencies of 50 Hz, 150 Hz, 250 Hz, 350 Hz, and 450 Hz.

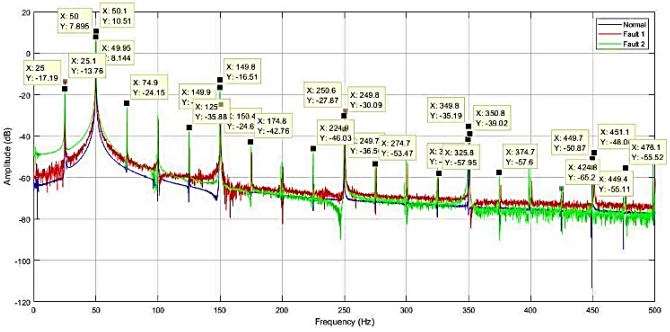

Fig. 8. Frequency spectrum normal and fault conditions

The average dB difference between the lowest sideband components and fundamental frequency components of all loaded conditions can be used as a reference for declaring fault detection, as shown in Fig. 9.

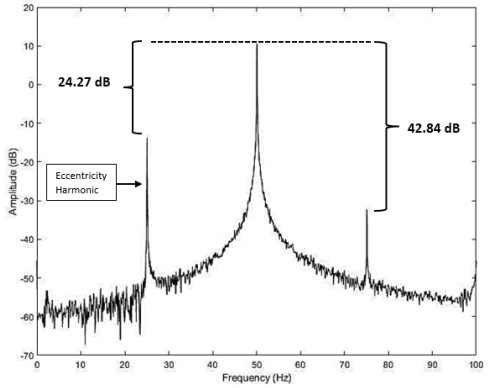

Fig. 9. Frequency spectrum fault conditions

The threshold is set by calculating the ranges between the upper and sideband harmonic amplitudes under all normal operating conditions. Potential interference is reported when the excitation harmonic amplitude is greater than the threshold during the testing period [15]. The following is a graph used as a normal motor's amplitude threshold.

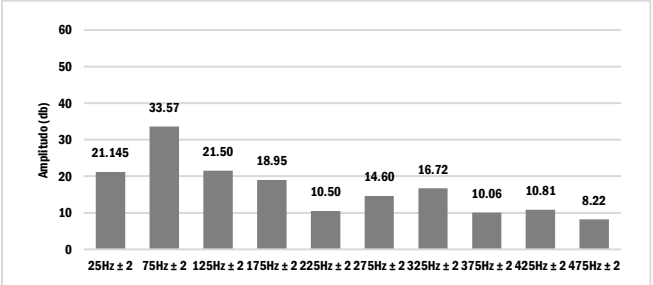

Fig. 10. The threshold of flux signal

A. *Spectrum Analysis on Balanced Condition*

In the frequency spectrum analysis, the results of normal motors in balanced conditions of no-load, half-load, and full-load were obtained. This made it easier to determine an increase in amplitude between normal and eccentricity motors. Fig. 11 shows the graphic of the eccentricity motor on balanced voltage conditions. Where eccentricity of 0.1 mm is shown in the red spectrum and eccentricity of 0.2 mm is shown in the green spectrum.

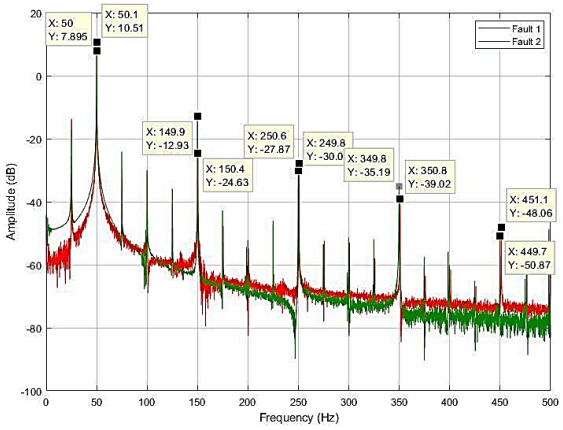

(a)

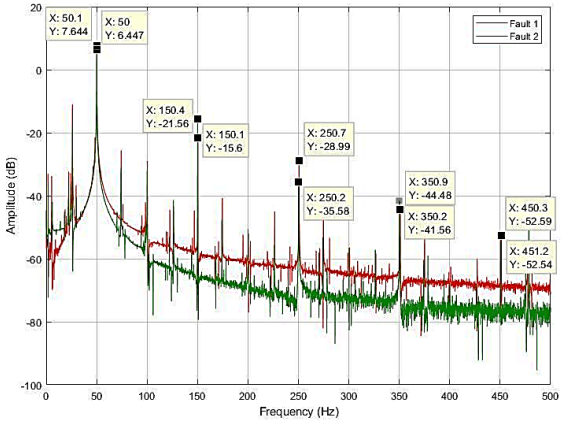

(b)

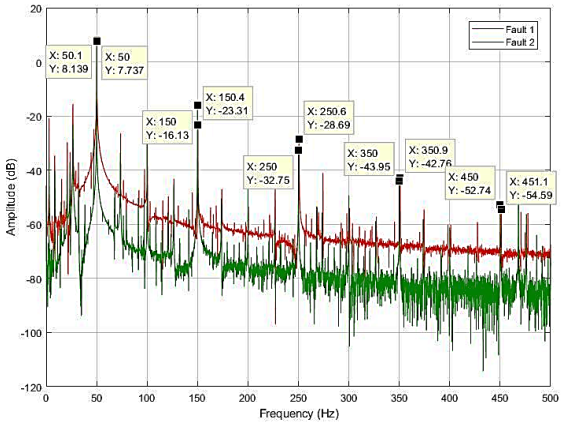

(c)

Fig. 11. Frequency spectrum eccentricity fault motor on balanced voltage conditions (a) no-load (b) half-load (c) full-load.

In Fig. 11, it can be seen that the eccentricities 0.1 mm and 0.2 mm have a frequency spectrum that is not much different in the no-load condition. But there is an increase in spectrum ripple as the load increases, such as in half-load and full-load conditions. From this figure can be analyzed the

detection of eccentricity on the motor amplitude the eccentricity motor exceeds the threshold, so it can be said that the flux signal measurement detects damage. The comparison amplitude in the balance voltage condition can be shown in Fig. 12.

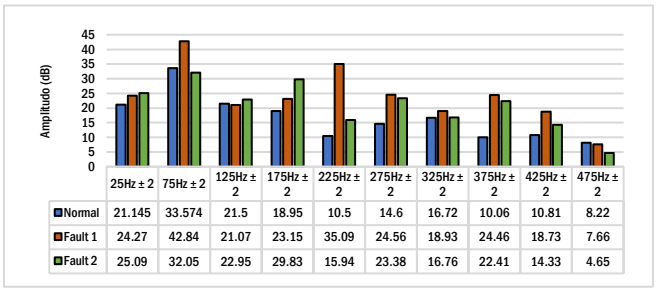

	25Hz ± 2	75Hz ± 2	125Hz ± 2	175Hz ± 2	225Hz ± 2	275Hz ± 2	325Hz ± 2	375Hz ± 2	425Hz ± 2	475Hz ± 2
Normal	21.145	33.574	21.5	18.95	10.5	14.6	16.72	10.06	10.81	8.22
Fault 1	24.27	42.84	21.07	23.15	35.09	24.56	18.93	24.46	18.73	7.66
Fault 2	25.09	32.05	22.95	29.83	15.94	23.38	16.76	22.41	14.33	4.65

(a)

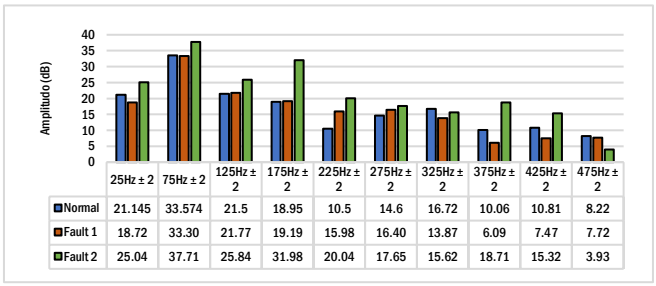

	25Hz ± 2	75Hz ± 2	125Hz ± 2	175Hz ± 2	225Hz ± 2	275Hz ± 2	325Hz ± 2	375Hz ± 2	425Hz ± 2	475Hz ± 2
Normal	21.145	33.574	21.5	18.95	10.5	14.6	16.72	10.06	10.81	8.22
Fault 1	18.72	33.30	21.77	19.19	15.98	16.40	13.87	6.09	7.47	7.72
Fault 2	25.04	37.71	25.84	31.98	20.04	17.65	15.62	18.71	15.32	3.93

(b)

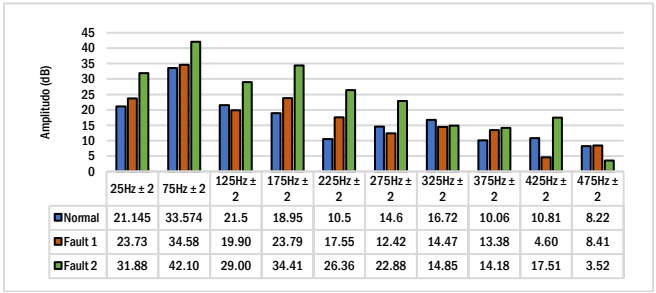

	25Hz ± 2	75Hz ± 2	125Hz ± 2	175Hz ± 2	225Hz ± 2	275Hz ± 2	325Hz ± 2	375Hz ± 2	425Hz ± 2	475Hz ± 2
Normal	21.145	33.574	21.5	18.95	10.5	14.6	16.72	10.06	10.81	8.22
Fault 1	23.73	34.58	19.90	23.79	17.55	12.42	14.47	13.38	4.60	8.41
Fault 2	31.88	42.10	29.00	34.41	26.36	22.88	14.85	14.18	17.51	3.52

(c)

Fig. 12. Comparison amplitude of normal and eccentricity fault motor in the balance voltage condition (a) no-load (b) half-load (c) full-load

Fig. 12 shows the highest amplitude value or the maximum number of all experiments with varying loads at an eccentricity of 0.1 mm (Fault 1) with values of 42.84 dB, 35.09 dB, 24.27 dB, 23.15 dB, 24.56 dB, 18.93 dB, 24.46 dB and 18.73 dB for experiments with no-load. In the half-load experiment, the amplitude was only four highest values that are 21.77 dB, 19.19 dB, 15.98 dB, and 16.40 dB, while in full-load, there were the six highest values that are 23.73 dB, 34.58 dB, 23.79 dB, 17.55 dB, 13.38 dB, and 8.41 dB. At an eccentricity of 0.2 mm (Fault 2), the highest amplitude was obtained for no-load experiments with values of 29.83 dB, 25.09 dB, 22.95 dB, 15.94 dB, 23.38 dB, 16.76 dB, 22.41 dB, and 14.33 dB. Afterward, the amplitude value increased by 25.04 dB, 37.71 dB, 25.84 dB, 31.98 dB, 20.04 dB, 17.65 dB, 18.71 dB, and 15.32 dB in the experiment with half-load. Meanwhile, in the full-load experiment, the eight highest amplitudes, with values are 31.88 dB, 42.10 dB, 29.00 dB, 34.41 dB, 26.36 dB, 22.88 dB, 14.18 dB, and 17.51 dB, were obtained. With this increase in amplitude, the result can be mentioned as damage identified.

B. Spectrum Analysis on Unbalanced Voltage Condition

The results showed differences in the frequency spectrum pattern of the eccentricity conditions. Fig. 12 shows a larger eccentricity frequency spectrum on balance voltage with loaded conditions than without load. Furthermore, the unbalanced voltage condition will be presented in Fig. 13 to describe the process of observing disturbances in the eccentricity spectrum by paying attention to the amplitude values. The unbalanced voltage with the test where the supply voltage on one of the phases is less than 5% or under voltage 5% is 209 V, and the other two phases are 220 V.

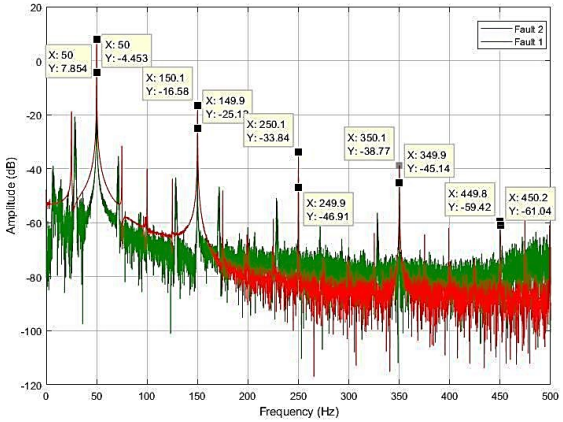

(a)

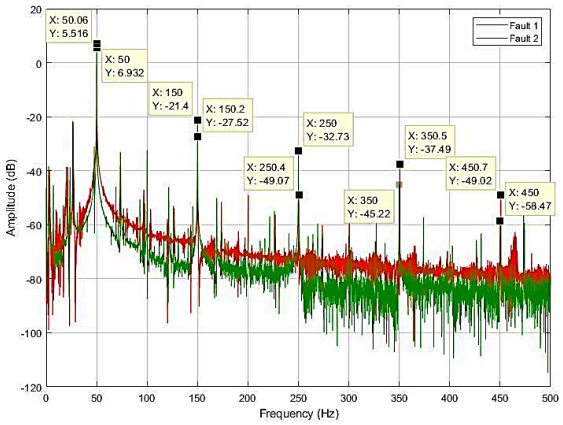

(b)

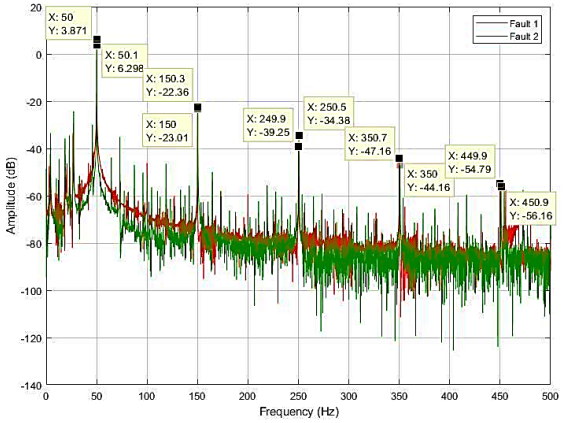

(c)

Fig. 13. Frequency spectrum eccentricity fault motor on unbalanced voltage conditions (a) no-load (b) half-load (c) full-load.

Fig. 13 presents the eccentricity frequency spectrum which the spectrum ripple is preponderant when it is no-load than load condition. It can be seen that the influence of unbalanced voltage can increase the eccentricity spectrum.

The results obtained on this eccentricity motor will be compared with the threshold value to ensure that damage is detected. A comparison amplitude of normal and eccentricity motors is visible in the graphic in Fig. 14.

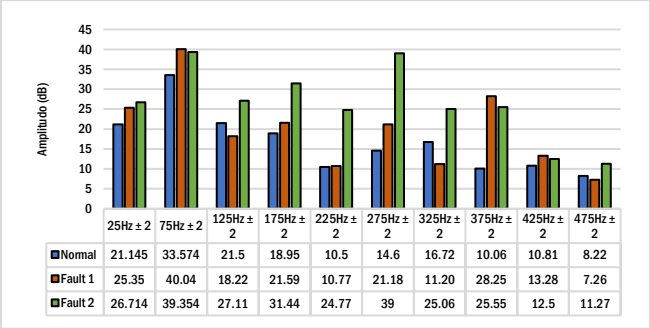

(a)

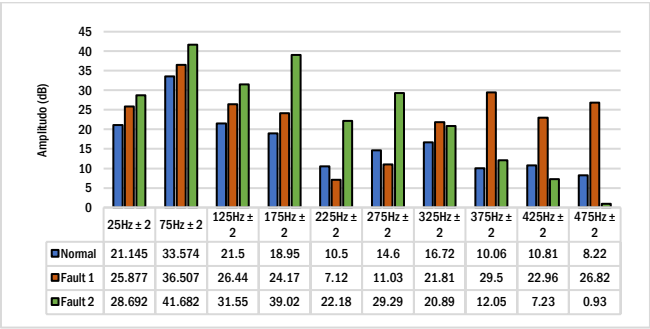

(b)

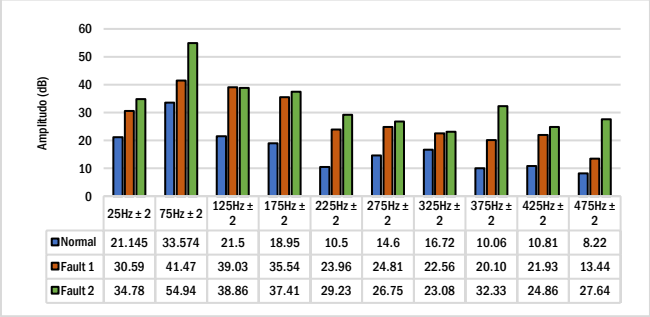

(c)

Fig. 14. Comparison amplitude of normal and eccentricity fault motor on unbalanced voltage conditions (a) no-load (b) half-load (c) full-load.

In the no-load unbalanced voltage experiment for eccentricity 0.1 mm (Fault 1), the seven highest amplitudes of 25.35 dB, 40.04 dB, 21.59 dB, 10.77 dB, 21.18 dB, 28.25 dB, and 13.28 dB were obtained. Meanwhile, in half-load, the amplitude was the highest, with values of 25.87 dB, 36.50 dB, 26.44 dB, 24.17 dB, 21.81 dB, 29.5 dB, 22,96 dB, and 26.82 dB. There is an increase in amplitude in full-load for eccentricity 0.1 mm (Fault 1) comprising 30.59 dB, 41.47 dB, 39.03 dB, 35.54 dB, 23.96 dB, 24.81 dB, 22.56 dB, 20.10 dB, 21.93 dB, and 13.44 dB.

In contrast to the eccentricity of 0.1 mm (Fault 1), in the no-load testing, there is the ten highest amplitude of 0.2 mm (Fault 2) with values 26.71 dB, 39.35 dB, 27.11 dB, 31.44 dB, 24.77 dB, 39 dB, 25.06 dB, 25.55 dB, 12.5 dB, and 11.27 dB. But the decrease occurred in the half-load test amplitudes were only the eight highest values which are 28.69 dB, 41.68 dB, 31.55 dB, 39.02 dB, 22.18 dB, 29.29 dB, 20.89 dB, and 12.05 dB. In the full-load testing, there were increases, highest amplitude values of 34.78 dB, 54.94 dB, 38.86 dB, 37.41, 29.23 dB, 26.75 dB, 23.08 dB, 32.33 dB, 24.86 dB, and 27.64 dB. From the spectrum analysis under unbalanced voltage conditions, it was found that more damage was detected and that amplitudes at the eccentricity frequency surpassed the threshold in normal motor conditions.

After comparing the eccentricity disturbance amplitude and the normal motor in all experimental conditions, the analysis results of the air gap eccentricity detection on the loaded and unloaded conditions carried out on voltage variations are shown in Table 3.

TABLE III. AMPLITUDE VALUES IN TESTING RESULT

Load	Eccentricity 0.1 mm (dB)		Eccentricity 0.2 mm (dB)	
	Balance	Unbalance	Balance	Unbalance
No Load	24.27	25.35	25.09	26.71
	42.84	40.04	-	39.35
	-	-	22.95	27.11
	23.15	21.59	29.83	31.44
	35.09	10.77	15.94	24.77
	24.56	21.18	23.38	39
	18.93	-	16.76	35.06
	24.46	28.25	22.41	25.55
	18.73	13.28	14.33	12.5
	-	-	-	11.27
Half Load	-	25.87	25.04	28.69
	-	36.50	37.71	41.68
	21.77	26.44	25.84	31.55
	19.19	24.17	31.98	39.02
	15.98	-	20.04	22.18
	16.40	-	17.65	29.29
	-	21.81	-	20.09
	-	29.5	18.71	12.05
	-	22.96	15.32	-
	-	26.82	-	-
Full Load	23.73	30.59	31.88	34.78
	34.58	41.47	42.10	54.94
	-	39.03	29.00	38.86
	23.79	35.54	34.41	37.41
	17.55	23.96	26.36	29.23
	-	24.81	22.88	26.75
	-	22.56	-	23.08
	13.38	20.10	14.18	32.33
	-	21.93	17.51	24.86
	8.41	13.44	-	27.64

After detected the eccentricity faults for all variations of the load on balanced and unbalanced voltage conditions, then the fault detection data is obtained that is combined in the table to determine the success in detecting eccentricity faults can be calculated using the equation below:

$$\% = \frac{the\ number\ of\ detected\ faults}{number\ of\ trials} \text{ x } 100 \qquad (6)$$

The results of the percentage of success in detecting interference are presented in Table 4.

TABLE IV. PERCENTAGE OF SUCCESS IN FAULT DETECTION

Load	Eccentricity 0.1 mm (%)		Eccentricity 0.2 mm (%)	
	Balance	Unbalance	Balance	Unbalance
No Load	80	70	80	100
Half Load	40	80	80	80
Full Load	60	100	80	100
Average	60	83,3	80	93,33

From Table 4, the results show that under balanced voltage conditions, the fault detection success is 80% at loading variation no-load. The percentage of success was fault detected in the eccentricity of 0.1 mm and 0.2 mm. At half-load, the rate of fault detection success decreased to 40% on the eccentricity of 0.1 mm, and there was no change with the eccentricity of 0.2 mm. When full load, fault detection success increases to 60% on the eccentricity of 0.1 mm, and on the eccentricity of 0.2 mm the percentage of success remains 80%. When the unbalanced voltage condition, the detection success increases to 100% on the eccentricity of 0.2 mm, and on the eccentricity of 0.1 mm eccentricity, the percentage of success decreases to 70% at no-load conditions. The success of detecting the eccentricity of 0.1 mm and 0.2 mm increases when the load changes to half-load with a success percentage of 80% and 100% at full-load conditions.

V. CONCLUSION

In this paper, a new diagnostic method is proposed, it is finding a threshold value from flux signal measurement data using a flux sensor, ELF *Gaussmeter*: IDR-210 with two levels of static eccentricity disturbance in the eccentricity variation modeled and analyzed. Then compare the spectrum data on normal and faulty motors, the eccentricity severity value, and compute the percentage of successful detection of the disorder analyzed. Detection is carried out on balanced and unbalanced voltage conditions with different loads. The success rate in this study is a better significant value of interference detection on average of almost 100%. Average fault detection of the eccentricity of 0.1 mm and 0.2 mm achieved 83.3% and 93.3% in unbalanced voltage conditions.

VI. REFERENCES

[1] N. R. Alham, D. A. Asfani, I. M. Yulistya N, and B. Y. A. N. Dewantara, "Analysis of Load and Unbalance Voltage on Air gap Eccentricity in detection of Three Phase Induction Motor," *Int. Conf. Inf. Commun. Technol.*, pp. 566–571, 2018.

[2] D. G. Dorrell, W. T. Thomson, S. Member, and S. Roach, "Analysis of Airgap Flux, Current, and Vibration Signals as a Function of the Combination of Static and Dynamic Airgap Eccentricity in 3-Phase Induction Motors," *IEEE Trans. Ind. Appl.*, vol. 33, no. 1, pp. 24–34, 1997.

[3] D. Hwang *et al.*, "Detection of air-gap eccentricity and broken-rotor bar conditions in a squirrel-cage induction motor using the radial flux sensor," *Am. Inst. Physics.*, vol. 131, no. 2008, pp. 129–132, 2012.

[4] M. Djamal, Suyatno, Yulkifli, and R. N. Setiadi, "SENSOR MAGNETIK FLUXGATE KARAKTERISTIK DAN APLIKASINYA," *J. Sains Mater. Indones*, pp. 207–214, 2007.

[5] F. E. Prahesti, D. A. Asfani, I. Made Yulistya Negara, and B. Y. Dewantara, "Three-Phase Induction Motor Short Circuit Stator Detection Using an External Flux Sensor," *Proc. - 2020 Int. Semin. Intell. Technol. Its Appl. Humanification Reliab. Intell. Syst. ISITIA 2020*, pp. 375–380, 2020.

[6] C. T. Kowalski and W. Kanior, "Effectiveness of the frequency analysis of the stator current in the rotor fault detection of induction motors," *Proc. IEEE Int. Conf. Ind. Technol.*, pp. 1–5, 2008.

[7] R. Romary, R. Corton, D. Thailly, and J. F. Brudny, "Induction machine fault diagnosis using an external radial flux sensor," *Eur. Phys. J. Appl. Phys.*, vol. 132, pp. 125–132, 2005.

[8] O. Vitek, M. Janda, V. Hajek, and P. Bauer, "Detection of eccentricity and bearings fault using stray flux monitoring," *SDEMPED 2011 - 8th IEEE Symp. Diagnostics Electr. Mach. Power Electron. Drives*, pp. 456–461, 2011.

[9] I. Nurhadi, A. I. Mahyuddin, and M. Ahmarudin, "Ciri Getaran Mekanik dan Arus Catu Pada Motor Listrik Induksi 3-Fasa Akibat Eksentrisitas Celah Udara." Departemen Teknik Mesin, FTI-ITB, Bandung, pp. 18–26, 1997.

[10] H. Henao, G.-A. Capolino, and C. Demian, "A Frequency-Domain Detection of Stator Winding Faults in Induction Machines Using an External Flux Sensor," *IEEE Trans. Ind. Appl.*, vol. 39, no. 5, pp. 1272–1279, 2003, doi: 10.1109/icit.2004.1490276.

[11] I. Ozelgin, "Analysis of magnetic flux density for airgap eccentricity and bearing faults," *Int. J. Syst. Appl. Eng. Dev.*, vol. 2, no. 4, pp. 162–169, 2009

[12] Hufri, Yulkifli, and M. Djamal, "Desain dan Pengembangan Sensor Magnetik Fluxgate Sensitivitas Tinggi Menggunakan Model Ellips-Multicore Double Pick-up dan Aplikasinya," Padang, 2009.

[13] S. M. A. Cruz and A. J. M. Cardoso, "Multiple reference frames theory: A new method for the diagnosis of stator faults in three-phase induction motors," *IEEE Trans. Energy Convers.*, vol. 20, no. 3, pp. 611–619, 2005, doi: 10.1109/TEC.2005.847975.

[14] R. M. Utomo, I. Made Yulistya Negara, D. A. Asfani, and N. R. Alham, "Wavelet Filter Selection Analysis for Air Gap Eccentricity in Three Phase Induction Motor," *Proceeding - 2018 Int. Semin. Intell. Technol. Its Appl. ISITIA 2018*, pp. 199–204, 2018.

[15] B. Yazici and G. B. Kliman, “An adaptive statistical time-frequency method for detection of broken bars and bearing faults in motors using stator current,” *IEEE Trans. Ind. Appl.*, vol. 35, no. 2, pp. 442–452, 1999.